Search for lensing signatures in gravitational-wave observations

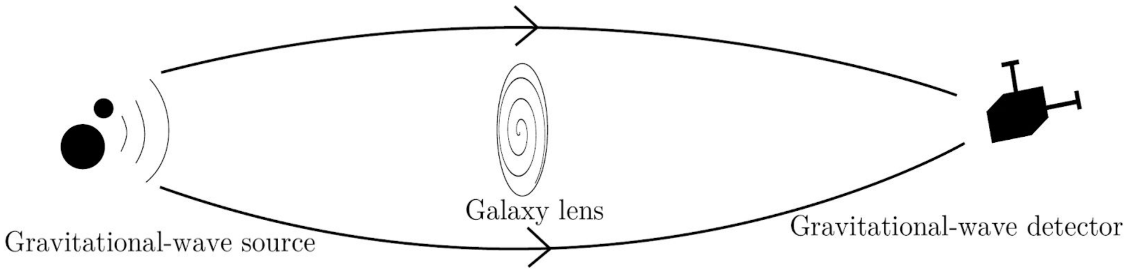


ESA/Hubble & NASA

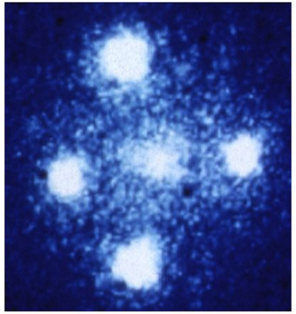
NASA, ESA, and STScI


NASA, ESA, Hubble SM4 ERO Team, ST-ECF

4th February 2022
CSGC, IIT Madras

On behalf of LVK lensing group

Presented by: Srashti Goyal (PhD Student, International Center for Theoretical Sciences, Bangalore)

Astronomy with gravitational lensing(bending) of light

- Look far
- Map Dark Matter
- Discover exoplanets

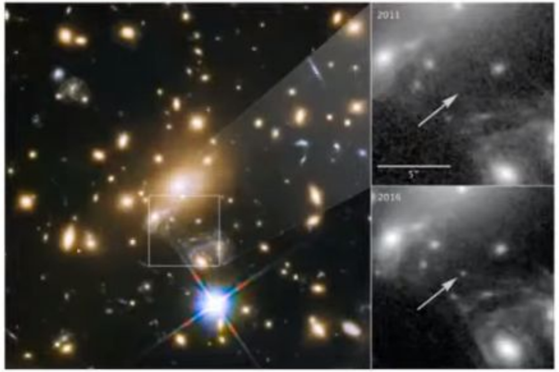

A distant star (right) at a distance of 9 billion light years is magnified more than 2,000 times by a galaxy cluster (right), making it visible from Earth.

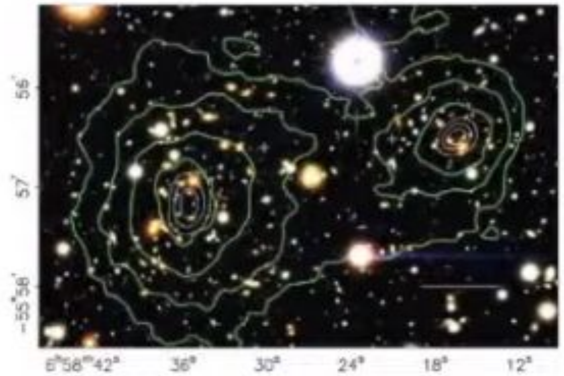

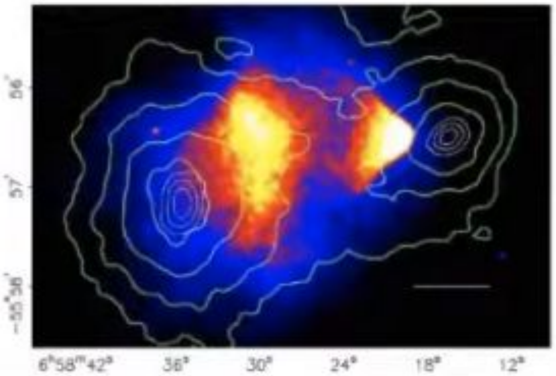

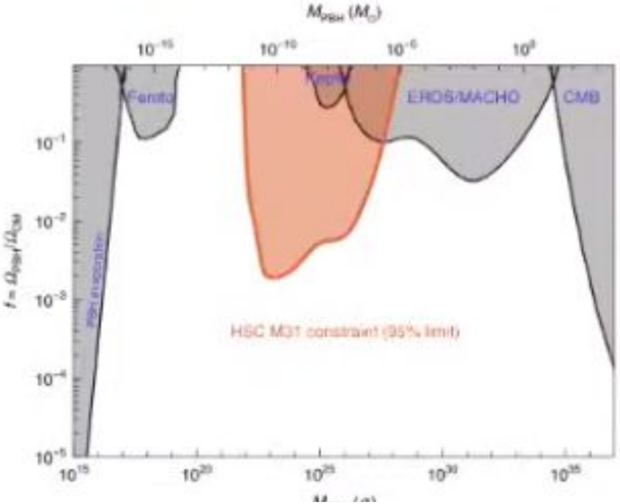

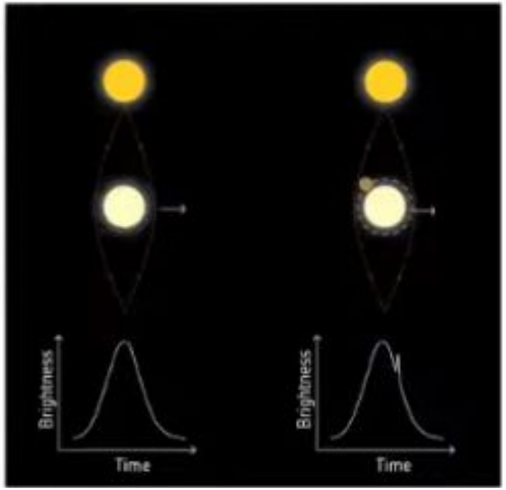

O3a: 1st LVC search of gravitational-wave lensing

Arxiv: [2105.06384]

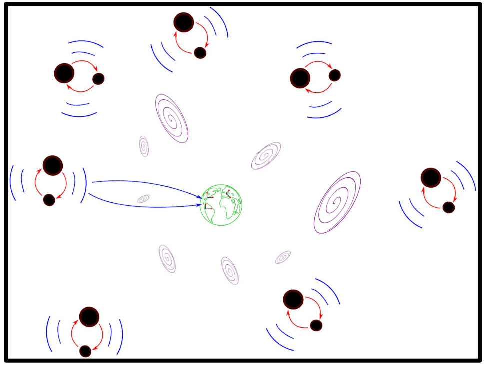

I. Lensing statistics

II. Lensing magnification

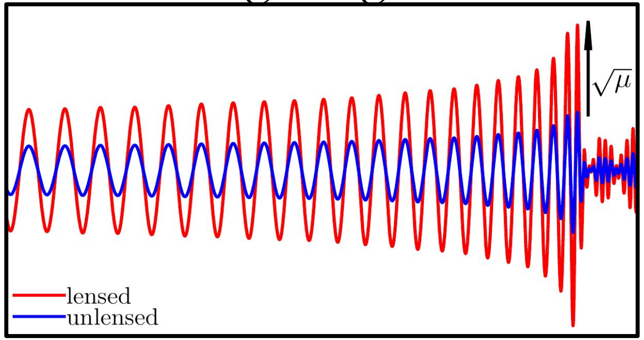

III. Multiple images

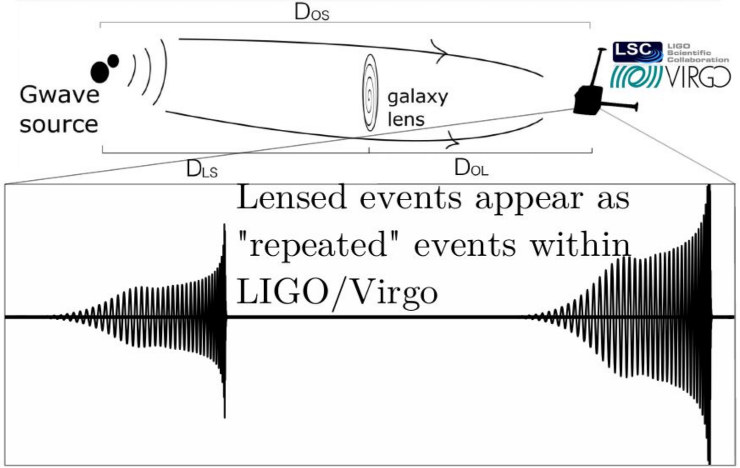

IV. Microlensing distortions

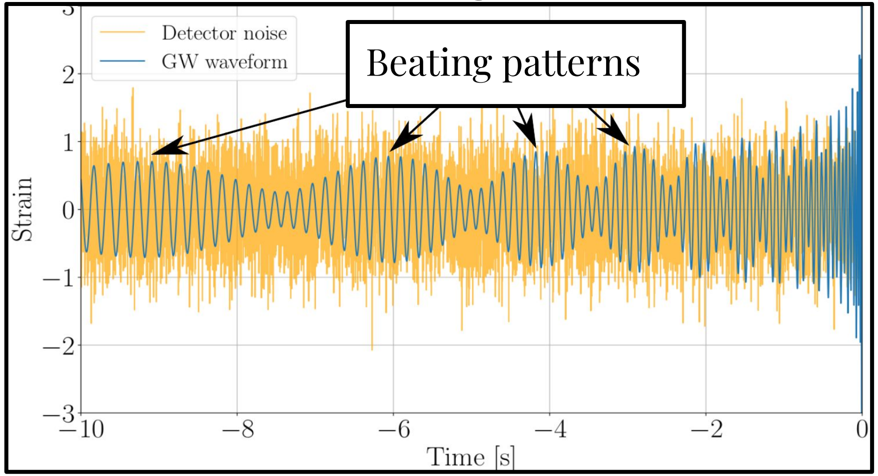

I. Lensing statistics (strong lensing)

- Given our understanding of
  - binary black hole population
  - lenses populations

We predict the rate of lensing

  - 1:$10^{3\text{-}4}$ events are expected to be lensed (vital for putting priors in follow up analyses)

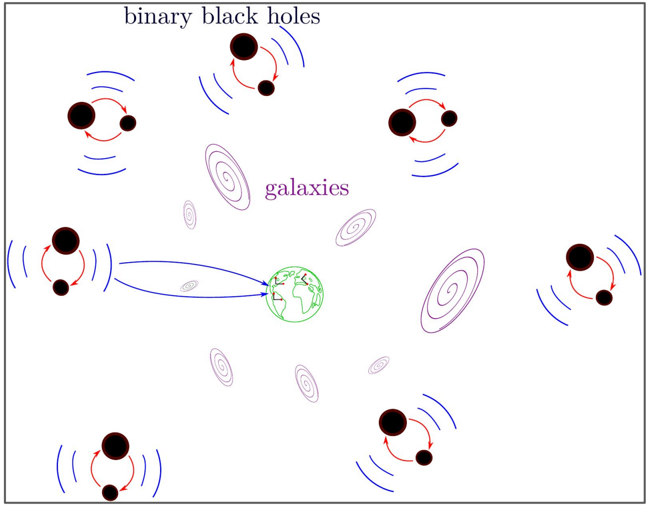

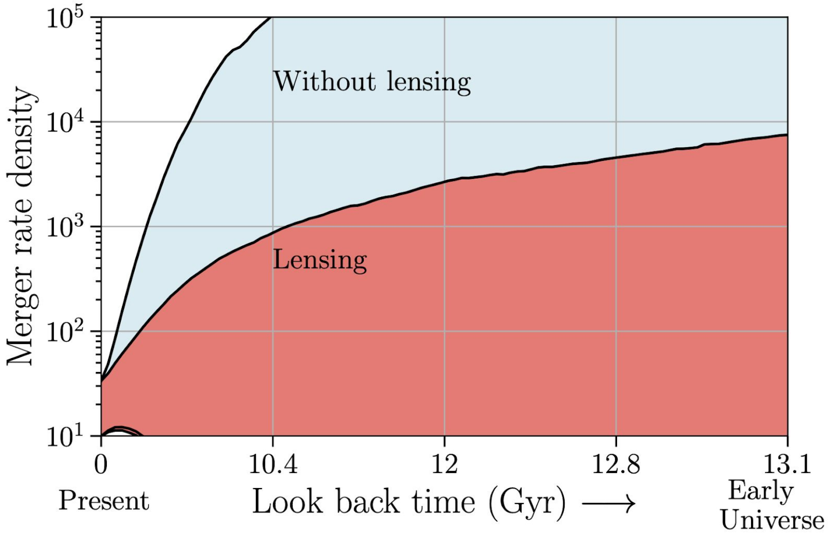

- Rate of mergers happening at early times are not well constrained currently

Non-detection of lensed events may help us to constrain models of merger rate densities at high redshifts

I. Lensing statistics (stochastic)

Implications on unresolvable CBCs from ***stochastic background searches..***

- Knowledge on detected CBCs from **population studies**
- Magnification model from Dai et al 2017: parametric fit to weak (Takahashi et al 2011) and strong regime (Hilbert et al 2008)
- Based on method in (Buscicchio et al 2020)

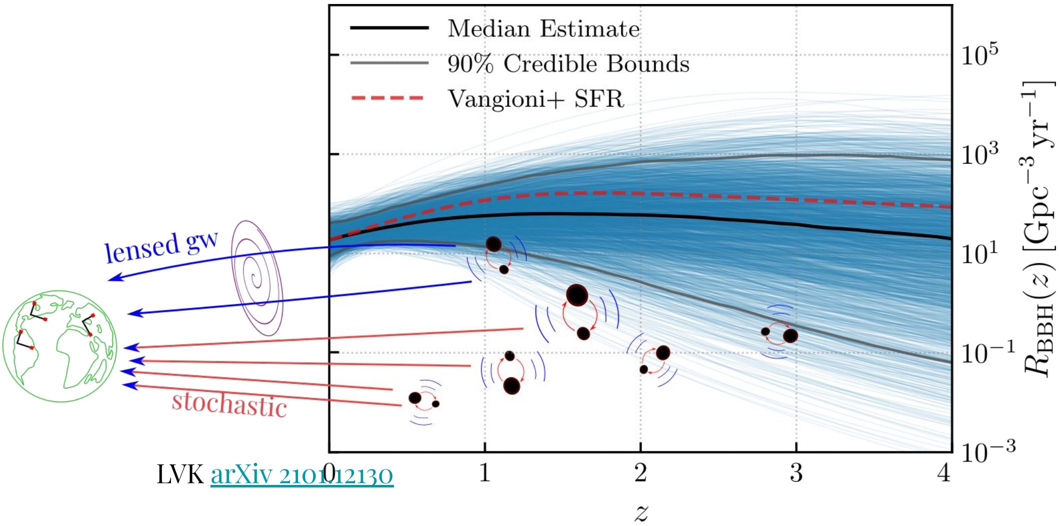

LVK arXiv 2101.12130

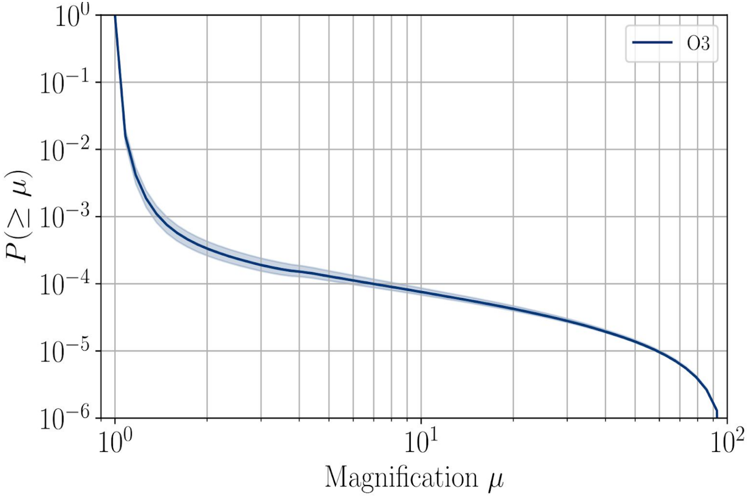

Conclusions

- Expected rate
  - $P(\mu>2) = 4:10^4$
  - $P(\mu>10) = 1:10^4$
- Merger rate rate uncertainties in blue shading

II. Lensing magnification

Lensing magnification can create apparently high-mass events..

- Analyze under the hypothesis that they originate from intrinsically lower-mass population:
  - Binary black holes with a mass gap at 50 or 65 solar masses
  - Binary neutron stars from the galactic double neutron star population

  Events analysed:-
  BNS: GW190425
  NSBH: GW190426_152155
  BBHs: GW190521, GW190602_175927, GW190706_222641

- Reported intrinsic source properties and expected magnification under the strong lensing hypothesis
  - BBHs: Moderate magnifications of order 10 originating from z~1-2,
    while BNS and NSBH would require high magnifications of order 100 or more.
- **No compelling evidence of lensing magnification. Important to categorise such events for follow up analysis.**

III. Search for multiple images

$$\tilde{h}_j^L(f;\theta,\mu_j,\Delta t_j,\Delta\phi_j) = \sqrt{|\mu_j|}\,h(f;\theta,\Delta t_j)\,e^{i\Delta\phi_j \mathrm{sign}(f)}$$

Magnification Time delay Morse phase

Image types:

Type I: minima $\Delta\phi_j=0$

Type II: saddle point $\Delta\phi_j=\pi/2$

Type III: maxima $\Delta\phi_j=\pi$

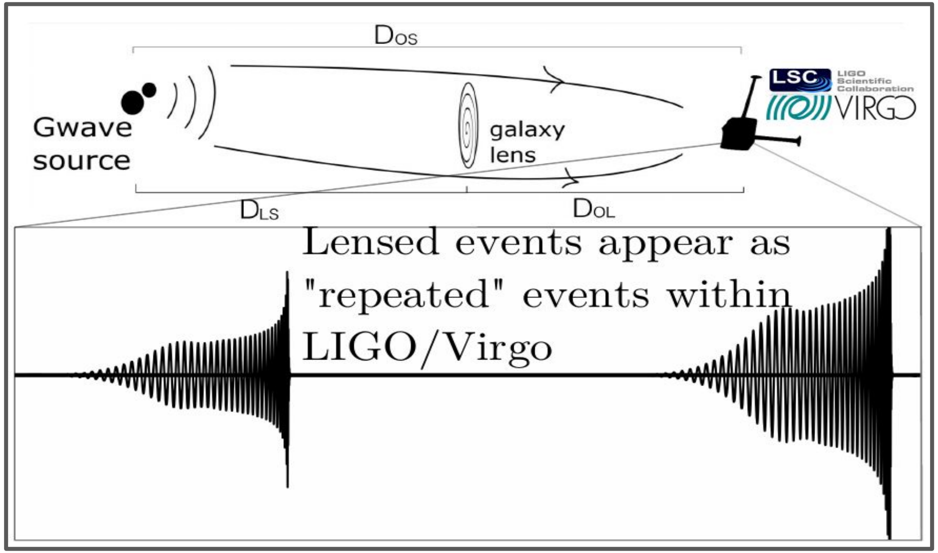

- The inferred luminosity distance and coalescence time would be different for lensed images of an event.
- While parameters such as masses, sky location and spins are expected to be the same for the two events
- Challenging to identify handful of lensed signals amongst thousands of unlensed ones.

IIIA. Posterior-overlap based multi-image analysis

[Haris et al., 2018]

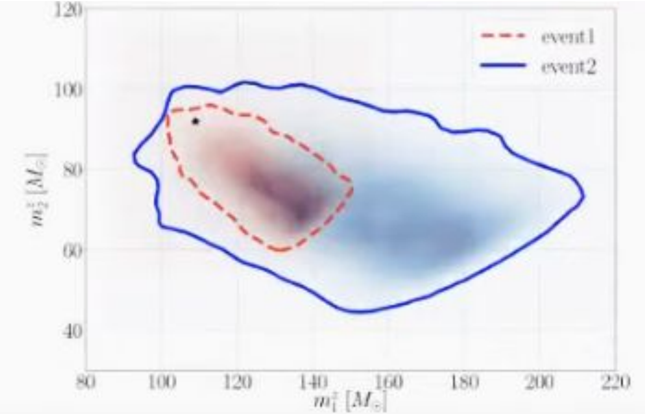

Check the consistency of posteriors between the pair of events.. fast!

Lensed hypothesis v/s unlensed hypothesis
for a selected pair of signals:

$$\mathcal{B}^{\rm overlap} = \int {\rm d}\Theta \, \frac{p(\Theta|d_1)\, p(\Theta|d_2)}{p(\Theta)} ,$$

$$\mathcal{R}^{\rm gal} = \frac{p(\Delta t|\mathcal{H}_{\rm SL})}{p(\Delta t|\mathcal{H}_{\rm U})},$$

Prior ratio of time delay distributions
(based only on galaxy lenses!)

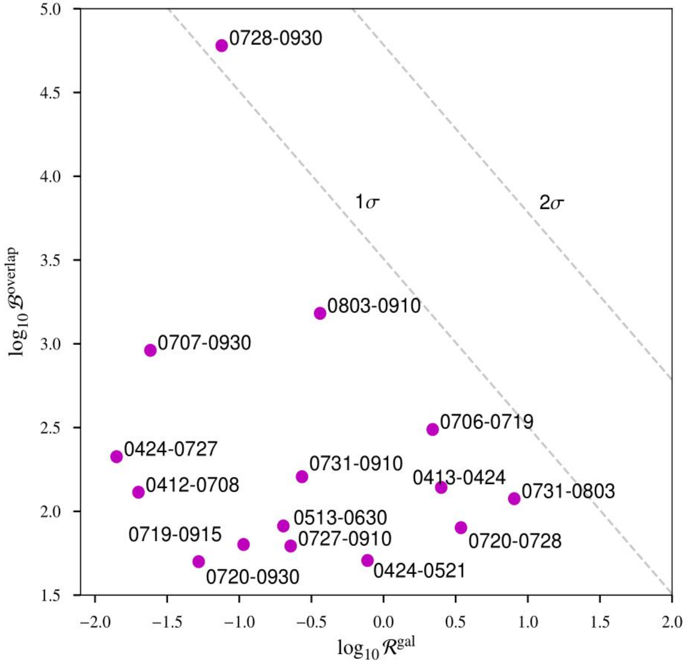

Using posteriors of 39 events, **19 event pairs with high bayes factors given to Joint-PE analysis.**

III.B joint parameter estimation analysis

This analysis includes information from the Morse phase which depends on the type of image… by the joint parameter estimation for the event pairs under the lensed hypothesis.

LALInference pipeline

[Methods paper Liu et al. 2020 (ApJ)]

- Aligned-spin quadrupole radiation included (IMRPhenomD, 11 param.)
- Morse phase equivalent to shift coalescence phase
- Treat each phase shift separately
- Applied to O1+O2 data

HANABI pipeline

[Methods paper Lo&Magaña 2021 (arXiv)]

- Higher modes + precession included (IMRPhenomXPHM, 15 param.)
- Morse phase added in frequency domain
- Sample over image types
- **Includes source and lens population priors**
- **Includes selection effects**

III.B Joint parameter estimation results

Event 1	Event 2	$\log_{10} \mathcal{R}^{\mathrm{gal}}$	$\log_{10}(C^{\mathrm{L}}_{\mathrm{U}})$ LALInference ($\Delta\phi$: 0, $\pi/2$, π, $3\pi/2$)	$\log_{10}(C^{\mathrm{L}}_{\mathrm{U}}\|_{\mathrm{pop}})$ HANABI	$\log_{10}(\mathcal{B}^{\mathrm{L}}_{\mathrm{U}})$ HANABI
GW190412	GW190708_232457	-1.7	(+1.0, -9.7, -22.8, -4.4)	-5.6	-8.0
GW190421_213856	**GW190910_112807**	–	(**+4.5**, +2.5, -1.5, -0.0)	0.67	**-1.8**
GW190424_180648	**GW190727_060333**	-1.9	(**+4.9**, +0.0, +1.1, **+4.0**)	0.96	**-1.5**
GW190424_180648	**GW190910_112807**	–	(+2.5, **+4.7**, **+4.3**, +1.6)	0.62	-1.8
GW190513_205428	**GW190630_185205**	-0.7	(+0.8, **+4.3**, -1.9, -6.5)	-0.39	-2.8
GW190706_222641	GW190719_215514	0.34	(+2.4, +2.4, -0.0, -0.5)	0.81	**-1.7**
GW190707_093326	GW190930_133541	-1.6	(-4.6, -4.3, -3.5, -4.1)	-8.2	-11.
GW190719_215514	**GW190915_235702**	-1.	(+3.5, -2.1, -0.1, **+4.1**)	1.4	**-1.1**
GW190720_000836	GW190728_064510	0.54	(-1.4, -0.9, -4.5, -5.4)	-6.0	-8.5
GW190720_000836	GW190930_133541	-1.3	(-3.5, -2.8, -3.9, -3.9)	-8.2	-11.
GW190728_064510	GW190930_133541	-1.1	(-3.6, -2.5, -3.1, -2.9)	-7.	-9.8
GW190413_052954	GW190424_180648	0.4	(+0.6, -0.9, +0.4, -0.0)	0.35	-2.1
GW190421_213856	**GW190731_140936**	-2.1	(+3.1, -1.9, +2.5, **+5.2**)	1.7	**-0.79**
GW190424_180648	**GW190521_074359**	-0.1	(+1.3, +3.8, +3.7, **+4.4**)	-0.64	**-3.1**
GW190424_180648	**GW190803_022701**	-2.1	(**+4.2**, +1.9, +2.6, +3.1)	0.81	**-1.7**
GW190727_060333	GW190910_112807	-0.6	(+1.8, +3.3, +3.7, +3.4)	0.12	-2.3
GW190731_140936	**GW190803_022701**	0.9	(**+4.1**, +3.2, +2.2, +3.4)	1.1	**-1.3**
GW190731_140936	**GW190910_112807**	-0.6	(+0.1, **+4.5**, +0.8, -7.2)	0.92	**-2.1**
GW190803_022701	**GW190910_112807**	-0.4	(**+4.0**, **+5.5**, **+4.7**, +2.6)	1.5	**-0.98**

Table 3

Coherence ratio: Overlap information

Population-weighted coh. ratio: overlap + prior BBH and lens population

Bayes factor: overlap + pop. prior + selection effects

No evidence of strongly lensed super-threshold pairs in GWTC-2

III.C Search for sub-threshold lensed images

Strongly lensed events could have ***fainter counterparts*** *not yet identified in wide parameter space searches..*

- Targeted searches can reduce the noise background thanks to a smaller trials factor when only looking for lensed waveforms that are identical up to the 3 points discussed before:

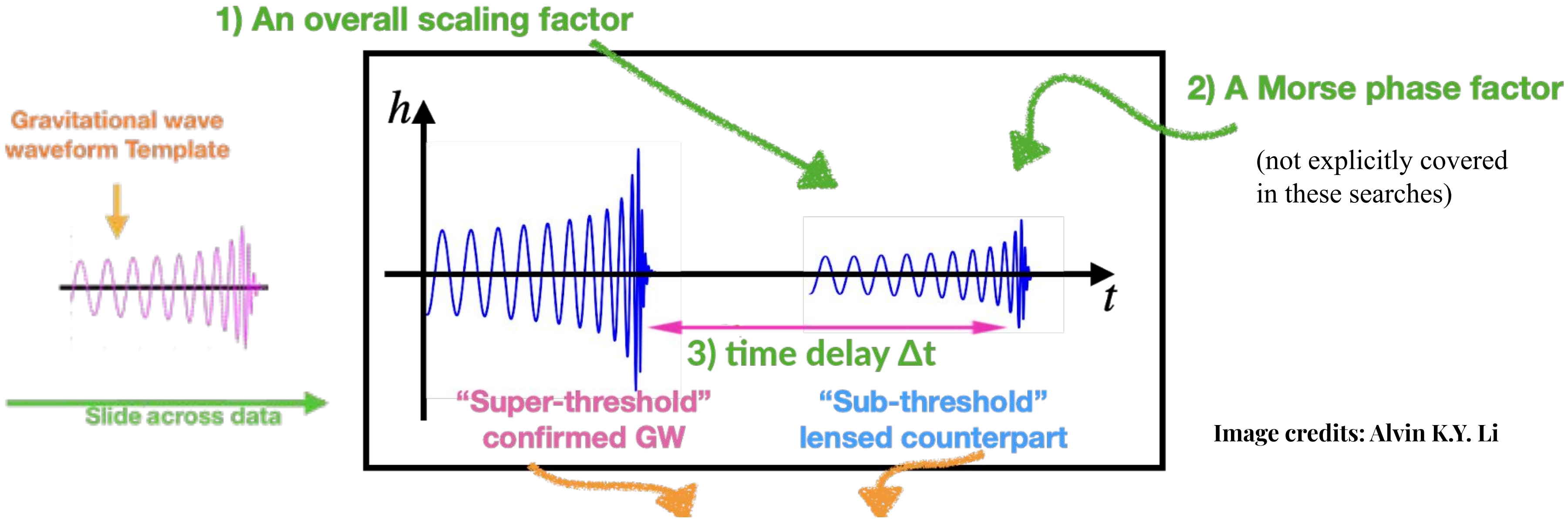

(not explicitly covered in these searches)

Image credits: Alvin K.Y. Li

They share similar intrinsic parameters!
(e.g. masses, spins…)

- Two matched-filter pipelines based on those already used in GWTC-2, two different targeted search strategies

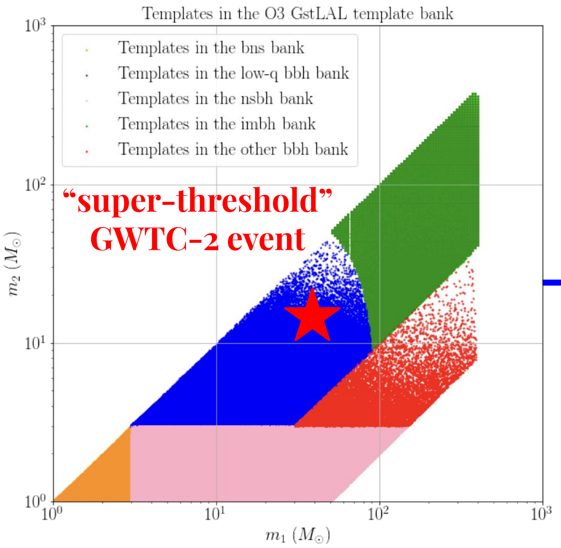

created based on Table II of GWTC-2

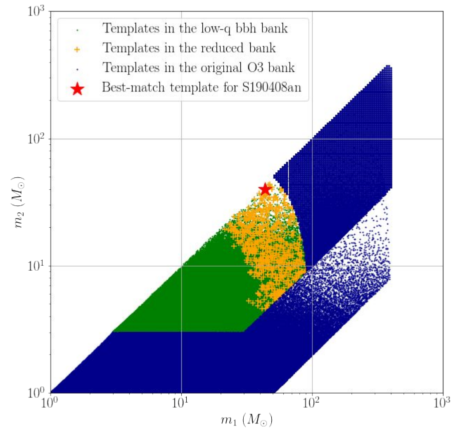

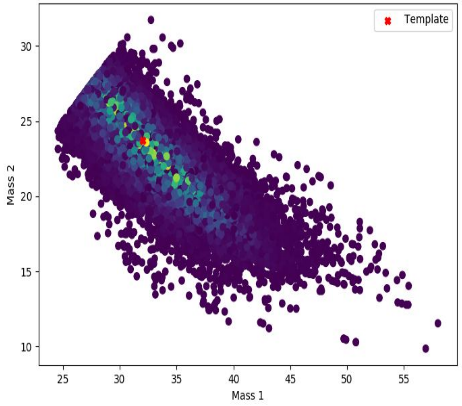

1) GSTLAL lensing search

- based on GSTLAL pipeline [Sachdev+2019; Hanna+2020; Messick+2017]
- lensing adaptation following Li+2019
- targeted template banks based on recovery of injections with parameters drawn from GWTC-2 posterior samples

2) PyCBC lensing search

- based on PyCBC pipeline [Nitz+2017]
- lensing adaptation following McIsaac+2019
- a single template per target (max-posterior of GWTC-2 samples)

figures for illustrative purposes only

III.C Search for sub-threshold lensed images

- ***8 new triggers found with FAR < 1/16 yr*** (6 of them unique)
- 6 candidate pairs followed up with LALInference joint PE *<u>assuming the triggers are astrophysical</u>* (we did not calculate a p_{astro} here for whether they are!)
- some pairs *consistent* with shared parameters, but compared with results shown before for GWTC-2 pairs, the obtained C^{L}_{U} give ***<u>no evidence</u>*** for lensed pairs

UTC time	GWTC-2 targeted event	$\|\Delta t\|$ [d]	$(1+z)\mathcal{M}$ [$M_\odot$]	FAR $[\mathrm{yr}^{-1}]$ PyCBC	FAR $[\mathrm{yr}^{-1}]$ GstLAL	$O_{90\%\mathrm{CR}}$ [%]	$\log_{10} C^{L}_{U}$ (LALInference) ($\Delta\phi$: 0, $\pi/2$, π, $3\pi/2$)
2019 Sep 25 23:28:45	GW190828_065509	28.69	17.3	0.003	98.681	0.0%	–
2019 Apr 26 19:06:42	GW190424_180648	2.04	65.5	–	0.017	63.8%	(−5.8, −5.8, −5.9, −5.6)
2019 Jul 11 03:07:56	GW190421_213856	80.23	47.7	0.032	0.341	1.2%	(+2.3, +1.1, +1.1, +2.6)
2019 Jul 25 17:47:28	GW190728_064510	2.54	9.0	–	0.038	0.0%	–
2019 Jul 11 03:07:56	GW190731_140936	20.46	47.4	0.045	0.944	2.9%	(+2.6, −1.2, −1.6, +0.9)
2019 Aug 05 21:11:37	GW190424_180648	103.13	68.8	–	0.051	26.9%	(−1.1, +0.6, −0.3, −0.7)
2019 Jul 11 03:07:56	GW190909_114149	60.36	49.0	0.053	1.196	12.6%	(+3.5, +2.2, +3.4, +2.9)
2019 Sep 16 20:06:58	GW190620_030421	88.71	53.3	0.055	1.389	49.5%	(+1.7, +3.6, +2.1, −3.2)

- last pair (highest C^{L}_{U}) has $\log_{10}(\mathcal{B}^{L}_{U}) = -3.2$ from Hanabi

IV. Microlensing search (wave-optics limit)

Microlenses which are comparable to the GW wavelength can modulate the waveforms by ***frequency-dependent amplification factors****…*

$$h^{ML}(f;\theta_{ML}) = h^{U}(f;\theta)\,F(f;M_L^z,y)$$

red-shifted lens mass **source position**

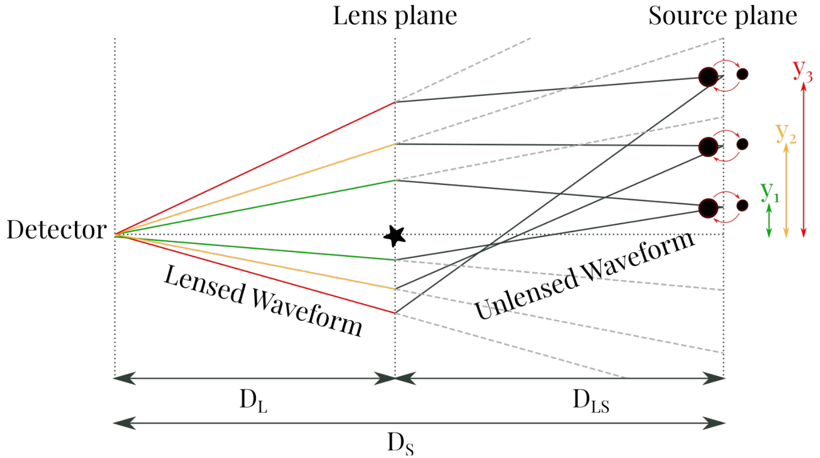

3 microlens systems with same M_L^z and different source positions

- Lensed images with time delays shorter than the chirp time of the signal superpose to create ***beating patterns*** which are more significant when the GW passes closer to the lens (ie. smaller ***y***).

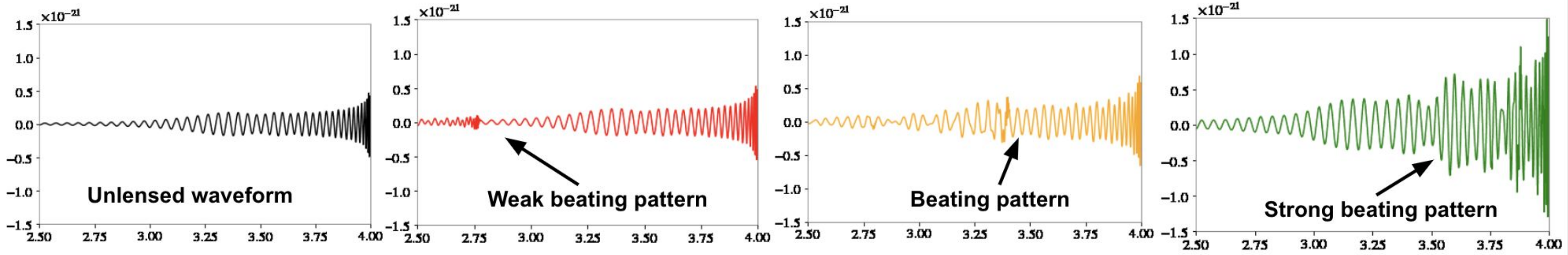

Search Method:

- Investigate lensing signatures due to **isolated point mass lens** on O3a events by calculating Bayes' factors between the two (lensed & unlensed) hypotheses.

Results:

- For none of the events are the posteriors well recovered, no high Bayes factors.
- Bayes factors for all events within the statistical fluctuations expected for unlensed events.
- **No microlensing effect observed.**

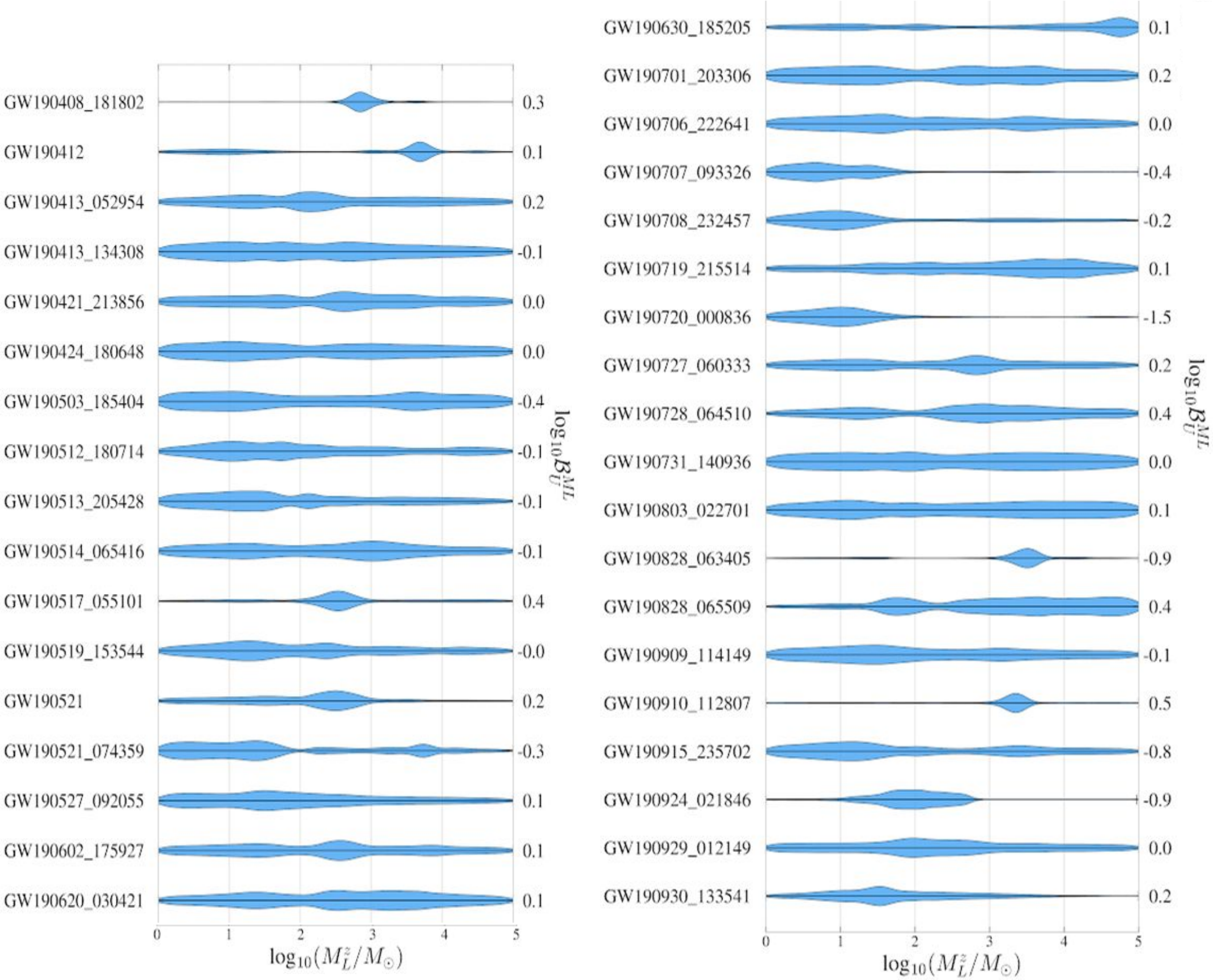

Conclusions

Four gravitational-wave analyses on O3a data:

- Statistical forecasts, constraining the rate of lensing
- Analysis of high-mass events under the hypothesis that they might be lensed
- Three searches for multiple images from strong lensing
- Search for microlensing-induced beating patterns

- First LVC analysis on a topic that is expected to be pursued further with new data (see the LVK white paper), **stay tuned for O3b lensing analysis.**

- As the current detector network expands and its sensitivity increases, our chances to detect lensing will improve.

Thank You for listening!